Anisotropic Rashba splitting of surface states from the admixture of bulk states: Relativistic *ab initio* calculations and *k·p* perturbation theory

E. Simon,[1,2] A. Szilva,[3] B. Ujfalussy,[1] B. Lazarovits,[1,3] G. Zarand,[3] and L. Szunyogh[3,*]

[1]*Institute for Solid State Physics and Optics, Hungarian Academy of Sciences, P.O. Box 49, H-1525 Budapest, Hungary*
[2]*Department of Physics, Lóránd Eötvös University, P.O. Box 32, H-1518 Budapest, Hungary*
[3]*Department of Theoretical Physics, Budapest University of Technology and Economics, Budafoki út 8., H-1111 Budapest, Hungary*

We investigate the surface Rashba effect for a surface of reduced in-plane symmetry. Formulating a *k·p* perturbation theory, we show that the Rashba splitting is anisotropic, in agreement with symmetry-based considerations. We show that the anisotropic Rashba splitting is due to the admixture of bulk states of different symmetry to the surface state, and it cannot be explained within the standard theoretical picture supposing just a normal-to-surface variation in the crystal potential. Performing relativistic *ab initio* calculations we find a remarkably large Rashba anisotropy for an unreconstructed Au(110) surface that is in the experimentally accessible range.

PACS number(s): 71.15.Rf, 73.20.At, 75.70.Tj

I. INTRODUCTION

Metallic surfaces often exhibit Shockley-type surface states located in a relative band gap of the bulk band structure and forming a two-dimensional electron gas. One of the most intriguing manifestation of spin-orbit coupling (SOC) at surfaces is the splitting of these surface states, known as Rashba splitting.[1,2] Such Rashba splitting was observed via photoemission by LaShell *et al.*[3] for the *L*-gap surface state at Au(111) and explained theoretically in terms of a tight-binding model[4] and *ab initio* electronic structure calculations[5,6] but several studies of the Rashba splitting were recently published in on Bi(111) and Bi/Ag(111),[7–9] as well as on Bi$_x$Pb$_{1-x}$/Ag(111), where atomic Bi *p* orbitals lead to a more pronounced spin-orbit splitting.[10–13]

Describing and controlling the Rashba splitting of surface states is crucial for spintronics applications. The famous Datta-Das transistor relies on the electric tuning of the Rashba splitting[14] and the Rashba splitting is responsible for the spin Hall effect in two dimensions[15] and the anomalous Hall effect[16] as well. A ferromagnetic control of the Rashba coupling has also been proposed very recently.[17]

The simplest way to understand the origin of the Rashba effect is to take nearly free electrons, confined by a crystal potential, $V(\mathbf{r}) = V(z)$, and having a plane-wavelike wave function, $\psi_{s,\mathbf{k}}(\mathbf{r}) = e^{i\mathbf{k}\mathbf{r}}\phi(z)\chi_s$, with χ_s some spinor eigenfunctions, and $\mathbf{k}$ the momentum parallel to the surface. The crystal potential $V(z)$ obviously produces an electric field, $\mathbf{E}$, perpendicular to the surface, which, in the presence of spin-orbit interaction leads to the following spin-orbit term in the effective Hamiltonian:

$$H_R(\mathbf{k}) = \alpha_R(k_x\sigma_y - k_y\sigma_x), \qquad (1)$$

called Rashba-Hamiltonian. In Eq. (1), σ_i denote the Pauli matrices and $\alpha_R = \frac{\hbar^2}{4m^2c^2}\int d^3r |\phi(z)|^2 \partial_z V(\mathbf{r})$ is the so-called Rashba parameter. The eigenvalue problem can then easily be solved, resulting in a splitting of the spin degeneracy of the surface states, $\varepsilon_\pm(\mathbf{k}) = \frac{\hbar^2}{2m^*}\mathbf{k}^2 \pm \alpha_R|\mathbf{k}|$, with m^* the effective mass of the surface electrons.[4,6] Clearly, the above dispersion is isotropic in k space, hence we term it as isotropic Rashba splitting.

Although real systems cannot be described in terms of free electrons, and for quantitative estimates of α_R the atomic structure of the potential needs be taken into account,[8] the form of the Rashba interaction, Eq. (1), is very robust for surfaces of high point-group symmetry such as C_{3v} or C_{4v}.[18]

The situation is, however, quite different for surfaces (or points in the surface Brillouin zone) of reduced symmetry. Such Shockley-type surface states emerge, e.g., around the $\bar{Y}$ point of the surface Brillouin zone of unreconstructed and (2×1) reconstructed Au(110) surfaces, as revealed by recent high-resolution photoelectron spectroscopy experiments.[19] In this case, the C_{2v} point-group symmetry of the system not only implies the asymmetry of the effective mass, $m_x^* \neq m_y^*$ (for the crystal axes see Fig. 1) but, in leading order in $\mathbf{k}$, representation theory also predicts the following simple form of the effective Hamiltonian:[18]
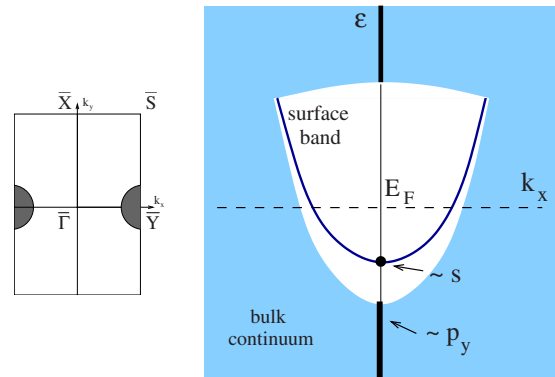

FIG. 1. (Color online) Left: sketch of the fcc(110) surface Brillouin zone. The dark area denotes the projection of the *L* gap of bulk Au. Right: structure of the surface energy spectrum in the absence of SO interaction, along the line $\mathbf{k} = (k_x, 0)$. Surface states in the relative gap with $\mathbf{k} \neq 0$ can be built up from states indicated by the thick black lines and the black circle at $\mathbf{k} = 0$. Note that $\mathbf{k} = 0$ corresponds to the $\bar{Y}$ point of the Brillouin zone, see Eq. (3).

$$H(\mathbf{k}) = \varepsilon_0 + \frac{\hbar^2 k_x^2}{2m_x^*} + \frac{\hbar^2 k_y^2}{2m_y^*} + \alpha_{R,x} k_x \sigma_y - \alpha_{R,y} k_y \sigma_x. \quad (2)$$

The above expression can easily be justified by simple symmetry analysis, just by noticing that σ_y and $-\sigma_x$ transform as p_x and p_y under the operations of the double groups of C_{2v} and C_{4v}. From this observation it also follows that in case of C_{4v} point-group symmetry $\alpha_{R,x} = \alpha_{R,y}$ must be satisfied, and Hamiltonian (1) is recovered.[20]

Although the above form of the Rashba interaction has been predicted in Ref. 18, no microscopic theory has been constructed so far to support it. While previous *ab initio* calculations[19,21] did find a Rashba splitting of the Au(110) surface state, they focused only on the dispersion along the $\overline{\Gamma}\overline{Y}$ direction, and therefore the anisotropy of the Rashba term remained unnoticed. In the present paper, we provide such a microscopic analysis for an Au(110) surface with C_{2v} point-group symmetry. First, constructing a $k \cdot p$ perturbation theory for the surface states we show that the above anisotropic Rashba structure appears naturally and is due to the finite momentum mixing of the bulk p states to the surface state. We also perform *ab initio* calculations of the Rashba-split surface state of an unreconstructed Au(110) surface and confirm with a high numerical accuracy that there is a large anisotropy in k space, $\alpha_{R,x} \sim 5\alpha_{R,y}$, in agreement with Eq. (2). The predicted anisotropic Rashba splittings turn out to be within the range of experimental accuracy.

II. $k \cdot p$ PERTURBATION THEORY OF THE RASHBA SPLITTING

Bloch states of Au(110) can be characterized by a surface momentum and can thus be written as

$$\psi_{\mathbf{Q}+\mathbf{k}}(\mathbf{r}) = e^{i\mathbf{k}\mathbf{r}} \phi_{\mathbf{Q},\mathbf{k}}(\mathbf{r}) \quad (3)$$

with the momentum $\mathbf{k}$ measured with respect to the momentum $\mathbf{Q}$ associated with the $\overline{Y}$ point of the surface Brillouin zone. Here the functions $\phi_{\mathbf{Q},\mathbf{k}}(\mathbf{r})$ are lattice antiperiodic in the x direction while they are lattice periodic in the y direction of the (110) plane, see Fig. 1. For any given momentum, $\mathbf{k}$, there exist an infinite number (continuum) of eigenstates, the energy of which ($\varepsilon_{\mathbf{k}}$) is determined by the condition that the states $\psi_{\mathbf{Q}+\mathbf{k}}$ be eigenstates of the Hamiltonian, $H = \frac{\mathbf{p}^2}{2m} + V(\mathbf{r}) + H_{SO}$, with H_{SO} denoting the spin-orbit coupling,

$$H_{SO}(\mathbf{r}) = \frac{\hbar}{4m^2c^2} [\nabla V(\mathbf{r}) \times \mathbf{p}] \sigma. \quad (4)$$

As a consequence, the functions $\phi_{\mathbf{Q},\mathbf{k}}$ must satisfy the equation,

$$\left[\frac{\mathbf{p}^2}{2m} + V(\mathbf{r}) + \frac{\hbar^2 \mathbf{k}^2}{2m} + \frac{\hbar}{m} \mathbf{k} \cdot \mathbf{p} + \widetilde{H}_{SO}(\mathbf{k},\mathbf{r}) \right] \phi_{\mathbf{Q},\mathbf{k}}(\mathbf{r})$$

$$= \varepsilon_{\mathbf{k}} \phi_{\mathbf{Q},\mathbf{k}}(\mathbf{r}) \quad (5)$$

with $\widetilde{H}_{SO}(\mathbf{k},\mathbf{r})$ being the effective SO coupling,

$$\widetilde{H}_{SO}(\mathbf{k},\mathbf{r}) = H_{SO}(\mathbf{r}) + \frac{\hbar}{4m^2c^2} [\nabla V(\mathbf{r}) \times \hbar\mathbf{k}] \sigma. \quad (6)$$

Similar to Bloch wave functions, for any fixed momentum, $\mathbf{k}$, (and for any value of $\widetilde{H}_{SO}$) the functions $\phi_{\mathbf{Q},\mathbf{k}}$ form a complete set for functions having the previously mentioned periodicity property. In the spirit of $k \cdot p$ perturbation theory, we can thus take the complete set of $\mathbf{k}=0$ and $\widetilde{H}_{SO}=0$ solutions, satisfying

$$\left[\frac{\mathbf{p}^2}{2m} + V(\mathbf{r}) \right] \phi_{i,n_i}(\mathbf{r}) = \varepsilon_{i,n_i} \phi_{i,n_i}(\mathbf{r}) \quad (7)$$

and expand $\phi_{\mathbf{Q},\mathbf{k}}$ in terms of these. Here we classified the solutions according to the four one-dimensional irreducible representations of the C_{2v} symmetry associated with the point $\overline{Y}$, $i \in \{1, x, y, xy\}$, and labeled solutions of a given symmetry by n_i. As shown in Fig. 1, the spectrum contains a discrete surface state of s symmetry and the projected bulk continuum forming the gap. Let us denote the $\mathbf{k}=0$ surface state by ϕ_0 and its eigenenergy by ε_0. Then states with $\mathbf{k} \neq 0$ but with $\widetilde{H}_{SO} \equiv 0$ can be expressed in terms of the states ϕ_{i,n_i} by performing second-order perturbation theory in $\mathbf{k}$, which amounts in a surface state

$$|\phi_{\mathbf{k}}^0\rangle = |\phi_0\rangle + \frac{\hbar}{m} \sum_{i,n_i(\neq 0)} \frac{|\phi_{i,n_i}\rangle\langle\phi_{i,n_i}|\mathbf{k} \cdot \mathbf{p}|\phi_0\rangle}{\varepsilon_0 - \varepsilon_{i,n_i}} \quad (8)$$

with approximate dispersion

$$\varepsilon_{\mathbf{k}}^0 = \varepsilon_0 + \frac{\hbar^2 k_x^2}{2m_x^*} + \frac{\hbar^2 k_y^2}{2m_y^*}, \quad (9)$$

$$\frac{1}{m_i^*} = \frac{1}{m} + \frac{2}{m^2} \sum_{n_i} \frac{|\langle\phi_{i,n_i}|p_i|\phi_0\rangle|^2}{\varepsilon_0 - \varepsilon_{i,n_i}} \quad (i = x, y). \quad (10)$$

The index 0 in $\varepsilon_{\mathbf{k}}^0$ and $|\phi_{\mathbf{k}}^0\rangle$ is meant to remind us to the absence of SO interaction.

To obtain the surface states, $|\phi_{\mathbf{k}}\rangle$, we then carry out first-order perturbation theory with the SOC operator, $\widetilde{H}_{SO}$, using the states $|\phi_{\mathbf{k}}^0\rangle$ as a starting point. Keeping just contributions linear in $\mathbf{k}$ we get two terms to the effective Rashba Hamiltonian. The second term in Eq. (6) gives rise to the usual isotropic Rashba model,

$$H_R^{iso}(\mathbf{k}) = \alpha_R (\mathbf{e}_z \times \mathbf{k}) \cdot \sigma \quad (11)$$

with $\alpha_R = \frac{\hbar^2}{4m^2c^2}\langle\phi_0|\partial_z V/\partial z|\phi_0\rangle$. The term H_{SO} in Eq. (6), however, gives also a finite contribution due to the admixture of $p_{x,y}$ states from the continuum and, in fact, this is precisely the term that leads to an anisotropic Rashba coupling,

$$H_R^{anis}(\mathbf{k}) = \frac{\hbar}{m} \sum_{i=x,y} k_i \sum_{n_i} \frac{\langle\phi_{i,n_i}|p_i|\phi_0\rangle(\langle\phi_0|\mathbf{a}|\phi_{i,n_i}\rangle\sigma) + \text{H.c.}}{\varepsilon_0 - \varepsilon_{i,n_i}}, \quad (12)$$

where we defined the (axial) vector operator related to SOC, $\mathbf{a} = \frac{\hbar}{4m^2c^2} [\nabla V(\mathbf{r}) \times \mathbf{p}]$. Using the symmetry of the unperturbed wave functions, a particularly simple form of the above an-

isotropic Rashba Hamiltonian can be obtained,

$$H_R^{\text{anis}}(\mathbf{k}) = \lambda_x k_x \sigma_y + \lambda_y k_y \sigma_x \qquad (13)$$

with the coefficient λ_x expressed as

$$\lambda_x = \frac{2\hbar}{m} \sum_{n_x} \frac{\text{Re}(\langle \phi_{x,n_x} | p_x | \phi_0 \rangle \langle \phi_0 | a_y | \phi_{x,n_x} \rangle)}{\varepsilon_0 - \varepsilon_{x,n_x}} \qquad (14)$$

and λ_y given by a similar expression. The structure of the combined terms, Eqs. (11) and (13), is identical to the one obtained by symmetry analysis, Eq. (2), with $\alpha_{R,x} = \alpha_R + \lambda_x$ and $\alpha_{R,y} = \alpha_R - \lambda_y$. It should be noted that Eq. (13) can be transformed into the familiar Rashba-Dresselhaus Hamiltonian used in the context of semiconductor quantum wells in the absence of bulk or interface inversion symmetry.[14,22,23] This formal similarity is due to the C_{2v} symmetry of the system, however, the mechanism described above is distinctly different from that leading to the Dresselhaus coupling, usually understood as a result of bulk inversion symmetry breaking,[14] completely absent in our system. Furthermore, increasing the in-plane symmetry of the potential (e.g., considering C_{4v} point-group symmetry imposing $\lambda_x = -\lambda_y$), the Dresselhaus coupling vanishes, whereas the term, Eq. (13), arising from the mixing of the surface state with bulk states, continues to contribute to the isotropic Rashba splitting.

III. AB INITIO CALCULATIONS FOR Au(110)

To obtain a quantitative estimate of the parameters $\alpha_{R,x/y}$ and the induced Rashba splittings, we performed calculations of the surface states of unreconstructed Au(110) surface near the $\bar{Y}$ point of the surface Brillouin zone, using the relativistic screened Korringa-Kohn-Rostoker method.[24] Noticeably, in this method no slab or supercell approach is used as the substrate is modeled by a perfect semi-infinite bulk system. The local spin-density approximation as parametrized by Vosko et al.[25] was applied, the effective potentials and fields were treated within the atomic sphere approximation (ASA) with an angular momentum cutoff of $\ell_{\max}=2$. The energy integrations were performed by sampling 16 points on a semicircular path in the upper complex semiplane and for the necessary k integrations we selected 64 k points in the irreducible segment of the surface Brillouin zone.

The computed dispersion relations along the $\bar{\Gamma}\bar{Y}$ (x) and the $\bar{Y}\bar{S}$ (y) directions are plotted in Fig. 2. The maximum binding energy, $\varepsilon_0 \simeq 370$ meV, is by about 200 meV less than the measured value[19] and other theoretical values.[19,21] This deviation is mostly caused by the ASA and the angular momentum cutoff, $\ell_{\max}=2$, which resulted in some error for the determination of the Fermi level and the vacuum potential.

The nearly free-electronlike, parabolic shape of the dispersion as well as the Rashba splitting being remarkably different along the two directions is obvious from Fig. 2, and a detailed analysis confirms this impression: the numerical results are very well fitted by the dispersions $\varepsilon_{\pm}(\mathbf{k}) = \varepsilon_0 + \frac{\hbar^2 k_x^2}{2m_x^*}$ $+ \frac{\hbar^2 k_y^2}{2m_y^*} \pm \sqrt{\alpha_{R,x}^2 k_x^2 + \alpha_{R,y}^2 k_y^2}$, obtained by diagonalizing the ap-
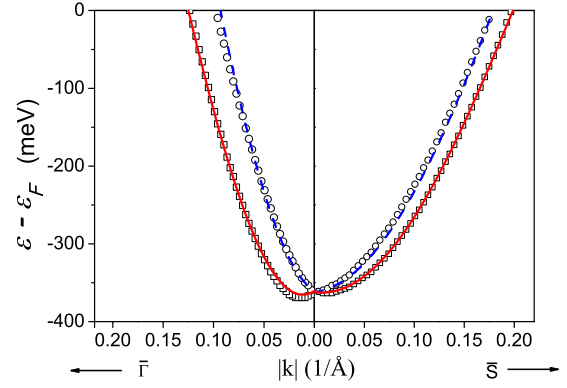

FIG. 2. (Color online) Dispersion relations of the Au(110) surface states at the $\bar{Y}$ point ($|k|=0$) along the $\bar{Y}\bar{\Gamma}$ and the $\bar{Y}\bar{S}$ directions. Symbols refer to the calculated data, solid and dashed lines to the fitted curves for $\varepsilon_-(\mathbf{k})$ and $\varepsilon_+(\mathbf{k})$, respectively.

proximate Hamiltonian, Eq. (2), with the fitting parameters, $m_x^* = 0.11m$, $m_y^* = 0.32m$, $\alpha_{R,x} = 0.8$ eV Å, and $\alpha_{R,y} = 0.17$ eV Å. The obtained effective mass along the $\bar{Y}\bar{S}$ direction is in satisfactory agreement with the measured value, $m_y^* = 0.25m$.[19] The effective mass along $\bar{\Gamma}\bar{Y}$, m_x^* is only about one third of m_y^*, which is the consequence that the states at the lower bulk band edge are mainly of p_z and p_x characters [see Eq. (9)]. Note that the energy separation of the surface state at the $\bar{Y}$ point is 0.8 eV and 3.4 eV with respect to the lower and upper bulk band edges, respectively, implying a strong admixture of "electron" states from the continuum below the surface state.

One of the most astonishing results of these numerical calculations is the remarkably large anisotropy of the Rashba parameters, $\alpha_{R,x} \sim 5\alpha_{R,y}$. In view of Eq. (14), this observation can also be explained with the absence of p_y states at the lower bulk band edge. This result also correlates with the results of the effective mass: the smaller value of m_x^* indicates a stronger admixture of p_x states, also responsible for the stronger renormalization of α_x.

In order to attest the above effect, it is worth to compare the Rashba splitting of the surface states for Au(110) with those of the well-established Au(111) case. From our corresponding calculations we conclude that $\alpha_{R,x}$ for Au(110) is even larger than α_R for the L-gap state of Au(111), 0.57 eV Å. This latter value is though considerably larger than the experimental one, 0.4 eV Å,[26] which correlates with the theoretically computed effective mass, $m^* \sim 0.19m_e$, being too small as compared to the experimentally observed value, $m^* \sim 0.25m_e$. The computed Fermi wave numbers, $k_F = 0.160$ and 0.189 Å^{-1}, on the other hand, are almost in perfect agreement with the measured values.[26] Nevertheless, based on the discrepancy regarding the value of the effective masses, we expect that our theoretical calculations for Au(110) somewhat overestimate the Rashba parameters, $\alpha_{R,x/y}$.

The anisotropic Rashba coupling together with the anisotropic effective mass gives rise to a Rashba-split Fermi surface for the surface states, as shown in Fig. 3. The Rashba splitting along $\bar{Y}\bar{S}$, $\Delta k_y \simeq 0.017$ Å^{-1} is in the order of the
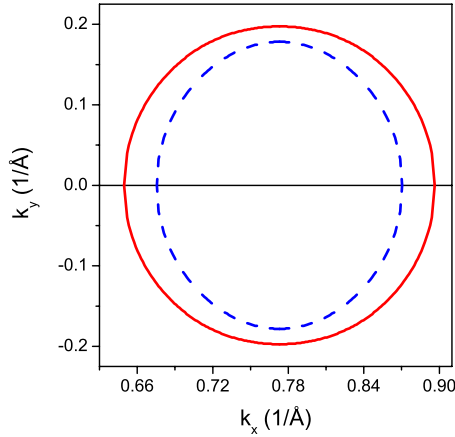
FIG. 3. (Color online) Rashba splitting of the Au(110) surface state at the Fermi level. Solid and dashed lines refer to the bands, $\varepsilon_+(\mathbf{k})$ and $\varepsilon_-(\mathbf{k})$, respectively.
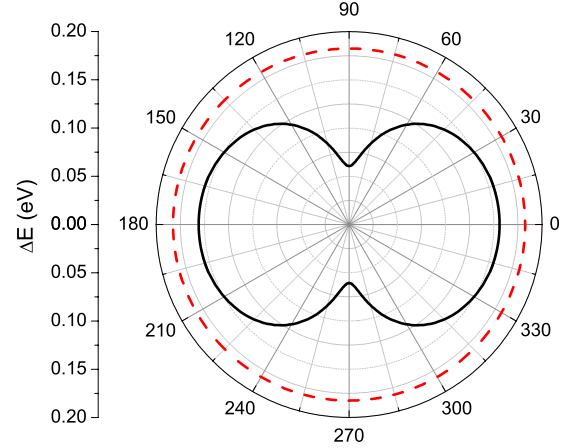

FIG. 4. (Color online) Energy differences, $\Delta\varepsilon(\mathbf{k}) = \varepsilon_+(\mathbf{k}) - \varepsilon_-(\mathbf{k})$, for the Rashba-split surface state of Au(110) (solid line) and Au(111) (dashed line) as a function of the polar angle $\varphi = \arctan\frac{k_y}{k_x}$, shown in units of degree around the graph. The magnitude of $\mathbf{k}$ was fixed to satisfy $\varepsilon_+(\mathbf{k}) = \varepsilon_F$. The energy scale is indicated by the axis on the left.

experimental resolution (0.01 Å^{-1}) (Ref. 19) but the value $\Delta k_x \simeq 0.026$ Å^{-1} implies that the Rashba splitting should be detectable experimentally along the $\overline{\Gamma}\overline{Y}$ direction.

In Fig. 4 we also show the polar plot of the energy splitting, $\Delta\varepsilon(\mathbf{k}) = \varepsilon_+(\mathbf{k}) - \varepsilon_-(\mathbf{k})$, between the two bands at the inner Fermi surface [$\varepsilon_+(\mathbf{k}) = \varepsilon_F$]. As a comparison, the same quantity is displayed for the surface state of Au(111). Supporting the above implication, $\Delta\varepsilon(\mathbf{k})$ along $\overline{Y}\overline{\Gamma}$ for Au(110) is almost as large as the (isotropic) energy splitting in case of Au(111). Furthermore, the extremely strong anisotropy of $\Delta\varepsilon(\mathbf{k})$, that could be inferred from angle-resolved photoemission experiments, is a clear fingerprint of the anisotropic Rashba effect discussed in this work.

IV. CONCLUSIONS

In summary, we constructed a $k \cdot p$ perturbation theory for surface states in the presence of SO coupling and derived a generalized Rashba Hamiltonian for (nearly free) electrons on metal surfaces. We found that in case of C_{2v} symmetry, the Rashba interaction gets an anisotropic part in first order of $\mathbf{k}$, which for Au(110) is found to dominate over the additional, well-known symmetric term. The anisotropic Rashba

term appears due to the mixing of the surface state with the bulk states for finite momenta. Even for surfaces of higher symmetry, this mechanism (i.e., the corresponding term in $k \cdot p$ perturbation theory) gives a large contribution to the isotropic part of the Rashba Hamiltonian. Our approach is rather general and—with minor modifications—can also be applied to other types of surface states with reduced symmetry.

Based on fully relativistic first-principles electronic structure calculations, we also demonstrated that a strongly anisotropic Rashba splitting should be experimentally observable for the unreconstructed Au(110) surface. It should, however, be mentioned that while a similar anisotropy of the Rashba splitting should pertain to the surface states of a missing-row reconstructed Au(110) surface, it could be more difficult to detect experimentally because these surface states lie above the Fermi level.[19]

*szunyogh@phy.bme.hu

[1] E. I. Rashba, Sov. Phys. Solid State **2**, 1109 (1960).

[2] Y. A. Bychkov and E. I. Rashba, JETP Lett. **39**, 78 (1984).

[3] S. LaShell, B. A. McDougall, and E. Jensen, Phys. Rev. Lett. **77**, 3419 (1996).

[4] L. Petersen and P. Hedegård, Surf. Sci. **459**, 49 (2000).

[5] G. Nicolay, F. Reinert, S. Hüfner, and P. Blaha, Phys. Rev. B **65**, 033407 (2001).

[6] J. Henk, A. Ernst, and P. Bruno, Phys. Rev. B **68**, 165416 (2003).

[7] Yu. M. Koroteev, G. Bihlmayer, J. E. Gayone, E. V. Chulkov, S.

Blügel, P. M. Echenique, and Ph. Hofmann, Phys. Rev. Lett. **93**, 046403 (2004).

[8] J. Premper, M. Trautmann, J. Henk, and P. Bruno, Phys. Rev. B **76**, 073310 (2007).

[9] C. R. Ast, J. Henk, A. Ernst, L. Moreschini, M. C. Falub, D. Pacilé, P. Bruno, Kl. Kern, and M. Grioni, Phys. Rev. Lett. **98**, 186807 (2007).

[10] G. Bihlmayer, S. Blügel, and E. V. Chulkov, Phys. Rev. B **75**, 195414 (2007).

[11] C. R. Ast, D. Pacilé, L. Moreschini, M. C. Falub, M. Papagno, K. Kern, M. Grioni, J. Henk, A. Ernst, S. Ostanin, and P. Bruno,

Phys. Rev. B **77**, 081407(R) (2008).

[12] T. Hirahara, T. Komorida, A. Sato, G. Bihlmayer, E. V. Chulkov, K. He, I. Matsuda, and S. Hasegawa, Phys. Rev. B **78**, 035408 (2008).

[13] J. H. Dil, F. Meier, J. Lobo-Checa, L. Patthey, G. Bihlmayer, and J. Osterwalder, Phys. Rev. Lett. **101**, 266802 (2008).

[14] For a review, see I. Žutić, J. Fabian, and S. Das Sarma, Rev. Mod. Phys. **76**, 323 (2004).

[15] J. Sinova, D. Culcer, Q. Niu, N. A. Sinitsyn, T. Jungwirth, and A. H. MacDonald, Phys. Rev. Lett. **92**, 126603 (2004); J. Wunderlich, B. Kaestner, J. Sinova, and T. Jungwirth, *ibid.* **94**, 047204 (2005).

[16] D. Culcer, A. MacDonald, and Q. Niu, Phys. Rev. B **68**, 045327 (2003); V. K. Dugaev, P. Bruno, M. Taillefumier, B. Canals, and C. Lacroix, *ibid.* **71**, 224423 (2005); T. S. Nunner, G. Zarand, and F. von Oppen, Phys. Rev. Lett. **100**, 236602 (2008).

[17] H. Mirhosseini, I. V. Maznichenko, S. Abdelouahed, S. Ostanin, A. Ernst, I. Mertig, and J. Henk, Phys. Rev. B **81**, 073406 (2010).

[18] T. Oguchi and T. Shishidou, J. Phys.: Condens. Matter **21**, 092001 (2009).

[19] A. Nuber, M. Higashiguchi, F. Forster, P. Blaha, K. Shimada, and F. Reinert, Phys. Rev. B **78**, 195412 (2008).

[20] Under C_{4v} or C_{3v} symmetries $\{\sigma_y, -\sigma_x\}$ transforms as an operator doublet while for C_{2v} the spin operators σ_y and σ_x correspond to different irreducible representations.

[21] M. Nagano, A. Kodama, T. Shishidou, and T. Oguchi, J. Phys.: Condens. Matter **21**, 064239 (2009).

[22] L. Vervoort, R. Ferreira, and P. Voisin, Phys. Rev. B **56**, R12744 (1997).

[23] U. Rössler and J. Kainz, Solid State Commun. **121**, 313 (2002).

[24] J. Zabloudil, R. Hammerling, L. Szunyogh, and P. Weinberger, *Electron Scattering in Solid Matter: A Theoretical and Computational Treatise* (Springer, Berlin, New York, 2005).

[25] S. H. Vosko, L. Wilk, and M. Nusair, Can. J. Phys. **58**, 1200 (1980).

[26] J. Henk, M. Hoesch, J. Osterwalder, A. Ernst, and P. Bruno, J. Phys.: Condens. Matter **16**, 7581 (2004).